Journal of Petroleum Science and Technology 13(3): 39, 2023, Pages 9-15
DOI: 10.22078/jpst.2024.5218.1900

Journal of Petroleum Science and Technology
Research Paper
https://jpst.ripi.ir/

Deactivation of Activated Alumina Adsorbents Used for H_2S Removal from Olefin-containing Streams

Sepehr Sadighi[1]*, Hossein Anisi[2], Yousefali Ghorbani[1] and Ali Karimi[1]
1. Catalysis Development Technologies Division, Research Institute of Petroleum Industry (RIPI), Tehran, Iran
2. Iran University of Science and Technology, School of Chemical, Petroleum and Gas Engineering, Tehran, Iran

Abstract
An oligomer produced from unsaturated and reactive components (green oil) is formed when hydrogen sulfide (H2S) is removed from the exhaust stream of the methyl tert-butyl ether (MTBE) plant. A remedy to minimize this contaminant formation is using adsorbents with low reactivity toward the olefinic precursors. Here, the green oil formation on the surface of different types of commercial alumina is studied. Results confirm that the regular commercially activated alumina has low H_2S adsorption capacity. Still, the alumina alkalized with 3.98 wt.% of Na_2O has a breakthrough time of more than 29 h and stable performance in a cyclic operation. Moreover, the promoted alumina with a wide pore diameter (about 9 nm) and low surface area (about 215 m^2/g) is less susceptible to deactivation by forming green oil. It is supposed that the capillary condensation of C_3/C_4 unsaturated compounds and acidic sites of the alumina intensify the oligomerization inside the pores of an adsorbent.

Keywords: Green Oil, Activated Alumina, Adsorption, Methyl tert-butyl ether, Hydrogen Sulfide.

Introduction
There are inflexible regulations regarding the emission of sulfur ingredients into the atmosphere. The presence of sulfur compounds is highly undesirable due to their impact on the environment and deteriorating effects on living souls [1-2]. Moreover, the corrosive nature of these compounds, especially hydrogen sulfide (H_2S), forces gas and oil refineries to use special materials, leading to a considerable increase in their capital expenditure [3]. These impurities always exist in the effluent stream of industrial processes [4-5], and the extra demand for crude oil and natural gas forces oil, gas, and petrochemical facilities to supply these commodities from sour wells in the future [6]. Therefore, they must more effectively eliminate sulfur compounds from their gas streams. This concern is crucial for the refineries supplied with Middle-Eastern crude oils [7].
Efficient methods are needed to eliminate such unwelcome guests from gas streams. There are many different approaches, such as absorption and adsorption, membrane and biological processes to eliminate H_2S from gas streams [8], and the use of adsorption techniques for removing pollutants, particularly sulfur ones, from waste streams have been proposed in recent years [9]. This process is usually performed in a fixed bed column consisting of adsorption and regeneration (or desorption) steps. The regeneration is usually carried out by raising the temperature (thermal swing adsorption, TSA) or reducing the operating pressure (pressure swing adsorption, PSA).
An important chemical compound produced from the dehydrogenation process is methyl tert-butyl ether (MTBE), which provides better combustion and increases the octane number of gasoline fuel [10]. To obtain isobutene for the production of MTBE, isobutane is dehydrogenated over a Pt-Sn/Al_2O_3 catalyst [11]. Due to the presence of unsaturated ingredients in the output stream of the MTBE reactor, an oligomer called green oil is formed when hydrogen sulfide (H2S) is adsorbed from the exhaust stream of the MTBE plant. This obnoxious side product is a mixture of C_4 to C_{20} unsaturated and reactive components with aliphatic dienes and olefins plus paraffins [12-13]. A low molecular weight fraction of the green oil vaporizes into the gas stream, and the heavier part deposits in the adsorbent pores, blocking micro and meso pores. It is obvious that shortening the life span of the adsorbent and fouling the downstream equipment are the consequences of this unfavorable side product.
Hence, it is momentous for any adsorbent to produce green oil as low as possible during adsorption, which is obtained by using adsorbents with low reactivity

**Corresponding author:* Sepehr Sadighi, *Catalysis Development Technologies Division, Research Institute of Petroleum Industry (RIPI), Tehran, Iran*
E-mail addresses: Sadighis@ripi.ir
Received 2024-01-29, Received in revised form 2024-03-03, Accepted 2024-03-05, Available online 2024-04-14

(acidity) towards the process stream [14-15]. Zeolites can be used as effective adsorbents with high stability and adsorption capacity due to their regular pores capable of size-, shape-, and polarity-based separation [16]. However, many researchers have reported that different adsorbents, especially zeolites, can potentially polymerize alkenes due to their high activity and good selectivity in various reactions [17-20]. Moreover, using alumina as the support of olefin polymerization is reported in the open literature, proving the affinity of this adsorbent for promoting side reactions to form green oil [21-22]. Consequently, pure alumina and zeolitic adsorbents are susceptible to oligomerizing unsaturated hydrocarbon, and their usage in petrochemical plants is restricted. Silico-alumino-phosphate (SAPO) sieves are also attractive due to their high adsorption capacity and selectivity towards light gases [23-24]. However, it has been reported that 40% of H_2S adsorbed by SAPO–43 at ambient temperature and pressure cannot be restored at low temperatures (180ºC) [25], which can limit the potential uses of SAPOs in the H_2S adsorption units.

Despite studies on polymerization and oligomerization of olefins and unsaturated hydrocarbons over alumina and zeolite adsorbents, few publications directly address the formation of the green oil on the surface and in the pores of alumina (the most popular adsorbent in oil, gas, and petrochemical industries), particularly for removing H_2S from the exhaust stream of an MTBE plant. Here, the formation of green oil on the surface of different commercial alumina adsorbents used for removing H_2S from the outlet gas stream of a MTBE plant is studied. This study is significant due to the catastrophic process problems caused by the green oil formation, specifically decreasing the life of adsorbents and fouling downstream facilities, resulting in the unplanned shut down of the gas purification unit.

Materials and Methods

Fig. 1 presents the simplified flow diagram of the setup used to study the performance of commercial alumina adsorbents. This pilot device was installed close to the target MTBE plant, and a part of the effluent stream leaving the industrial scale MTBE reactor with the gas hourly space velocity (GHSV) of 125 h^{-1} was introduced in the downward direction. The feed and operating conditions for the adsorption experiments are presented in Table 1. After the end of each adsorption stage, the adsorption bed was regenerated using a high-content hydrogen stream (see Table 2) at the GHSV of 228 h^{-1} in the upward direction. Three commercial adsorbents were used for sample studies; Sample A was a regular commercial activated alumina, and Samples B and C were promoted or alkalized commercial activated alumina. The physical characteristics of all adsorbents are revealed in Table 3.

Due to the presence of water in the feed stream and the possibility of losing the activity of the adsorbent, a regular type of molecular sieve 3A is provided at the top of the alumina layer (main bad) to prevent water ingression. The specifications of this molecular sieve are presented in Table 4.

Sulfur contents of the feed stream and treated product were analyzed using several Drager short-term tubes. Alumina adsorbents were analyzed using the X-ray fluorescence (XRF) method using the EDX XR-300 and WDX 1410 devices manufactured by Link Analytical and Philips companies, respectively. Powder X-ray diffraction (XRD) measurements of samples were conducted using a Philips PW1840 X-ray diffractometer with monochromatized Cu/Ka radiation (λ = 1.5406 nm). Micromeritics Tristar 3020 device was applied to analyze pore volume and size distribution using the nitrogen adsorption method. These experiments were repeated twice to confirm the reliability and repeatability. Furthermore, the green oil mass ratio of carbon to hydrogen (C/H) was analyzed according to the ASTM D5291 standard procedure. For an accurate justification, the geometry of the bed and operating conditions such as gas velocity, the particle size of adsorbents and the time of cycles, were selected, similar to the studied industrial adsorption process.

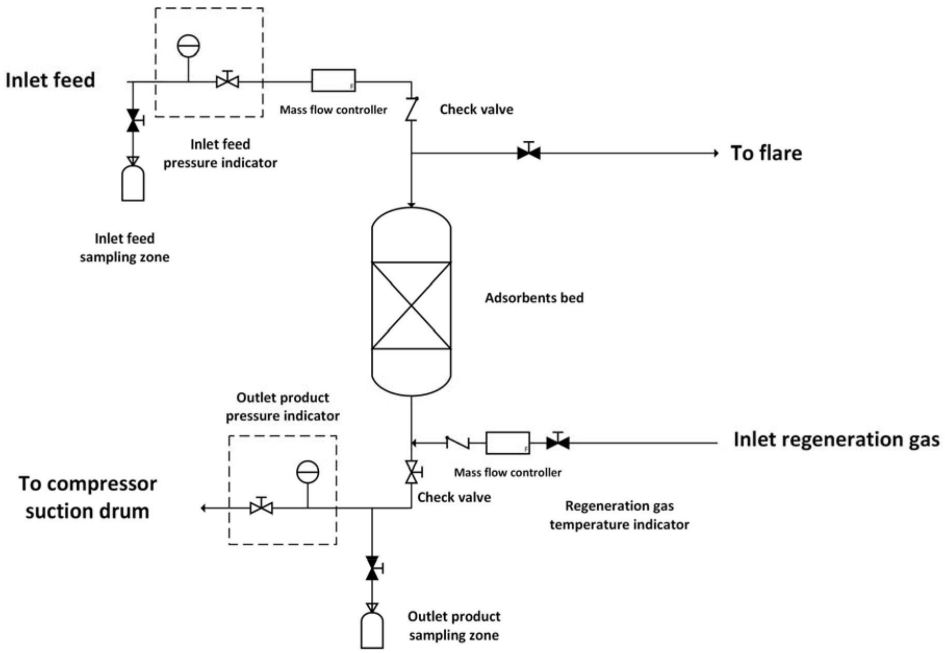

Fig. 1 Simplified schematic diagram of the pilot adsorption plant.

Table 1 Operating conditions and composition of the feed.

Feed operating conditions		
Conditions	Unit	Value
Temperature	°C	45
Pressure	barg	7.5
Mass flow rate	kg/h	106
Feed composition		
Components	Value (mol %)	
H_2	50	
CO	0.1	
CO_2	0.0015	
HCl	0.001 – 0.0015	
CH_4	3.1	
C_2H_6	0.1	
C_3H_8	0.9	
C_3H_6	0.5	
i-C_4H_{10}	28	
N-C_4H_{10}	0.6	
Trans 2-C_4H_8	0.2	
1-C_4H_{10}	0.1	
Cis 2-C_4H_8	0.2	
i-C_4H_8	15.5	
Neo-C_5H_{12}	0.16	
i-C_5H_{12}	0.25	
n-C_5H_{12}	0.05	
1,3 Butadiene	0.022	
C^{6+}	0.005	
H_2S	0.004 – 0.007	
H_2O	0.001 – 0.0015	

Table 2 Operating conditions and composition of the regeneration gas.

Regeneration gas operating conditions		
Temperature	°C	220
Pressure	barg	1.8
Mass flow rate	kg/h	4
Regeneration gas composition (mol%)		
H_2	94	
CH_4	5.89	
CO	0.11	
CO_2	0.0035	

Table 3 Physical specifications of alumina adsorbents.

Properties	Unit	Sample A	Sample B	Sample C
Shape	--	Beads	Beads	Beads
Diameter	mm	2-5	2-5	2-5
Bulk density	g/ml	0.70	0.75	0.74
Crush strength	N	140	160	166
BET surface area	m2/g	427.1	351.1	271.8

Table 4 Specifications of the molecular sieve 3A.

Properties	Unit	Value
Shape	--	Pellets
Diameter	mm	1.5 – 1.8
Bulk density	g/ml	0.68
Crush strength	N	45
Static water adsorption (@10 % R.H. & 25 ºC)	wt.%	19.5

As shown in Fig. 2, all experiments were carried out with 7 kg of the molecular sieve as the water guard bed and 60 kg of alumina adsorbent as the main bed. For all experiments, the heights of the 3A molecular sieve and alumina layers of the adsorption column were 0.141 m and 1.1 m, respectively. Moreover, to homogenously distribute the feed throughout the bed and avoid bed expansion, the top and bottom of the bed were packed with 100 mm of ¾ inch inert balls. At the start of the run, the bed was pretreated under the regeneration gas flow for 6 h at 220 °C in the upward direction, and then it was cooled. Afterward, the MTBE effluent gas was fed to the adsorption column.

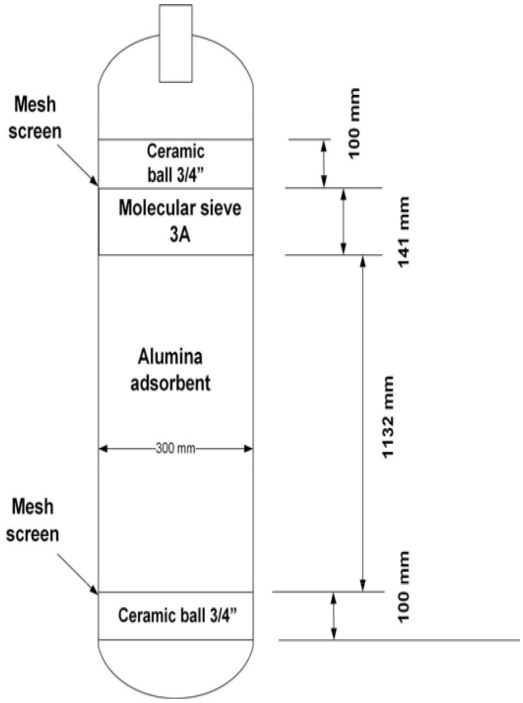

Fig. 2 Arrangement of the pilot scale adsorption column.

Results and Discussions

At first, to investigate the stability of adsorbents during the regeneration steps, an aging experiment was performed on the pure alumina (Sample A). Fig. 3 shows XRD analysis results for the fresh and aged adsorbents (calcination at 550°C for 4 h). As seen, the peaks at 14.3, 28.20, 37.95, 49.26, and 67.11º observed in the fresh adsorbent are related to boehmite and active alumina (γ, η, and ρ) phases. After the aging process, boehmite peaks at 14.3 and 28.2º disappeared due to the high temperature of the aging process and the conversion of boehmite to different types of alumina phases. By comparing the spectrum of the fresh and aged pure alumina adsorbents, it is concluded that no considerable crystal deformation in the alumina phase is observed. Because of impregnating and dispersing sodium oxide (Na_2O) on the surface of activated alumina, it is supposed that no peak of Na-oxide is detectable. Therefore, the same behavior can be observed for the promoted alumina [26]. Consequently, all alumina samples can be stable during the regeneration process, and the desorption temperature does not affect their crystallinities.

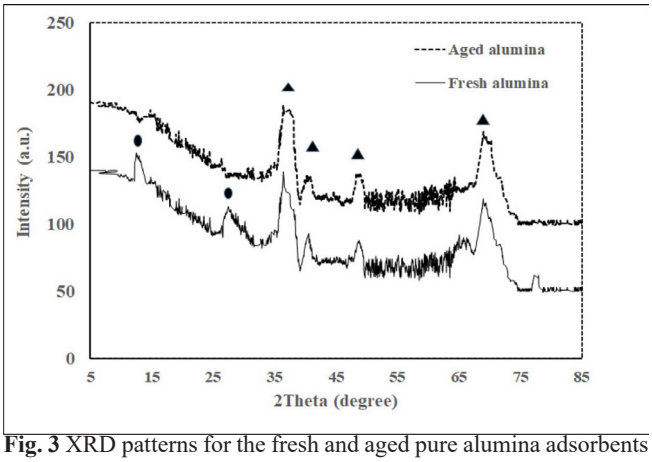

Fig. 3 XRD patterns for the fresh and aged pure alumina adsorbents (Sample A).

Fig. 4 represents the breakthrough time of the studied adsorbent for removing H_2S from the effluent stream of the MTBE reactor. The H_2S adsorption capacity of regularly activated alumina (sample A) is considerably lower than that of the promoted alumina in samples B & C. The elemental compositions of all samples are determined using the XRF technique to justify this observation. As reported in Table 5, the sodium content of the regular activated alumina in the form of sodium oxide (Na_2O) is significantly lower than the promoted ones. Furthermore, by increasing the Na_2O content from 3.73 wt.% to 3.98 wt.%, the H_2S adsorption capacity increases from about 27 wt.% (Sample B) to 30 wt.% (Sample C). Therefore, sodium impregnated on adsorbents by using sodium hydroxide [27] is the main feature for enhancing the adsorption capacity of sulfur compounds on the alumina surface through the following reaction:

$$NaOH+H_2S \rightarrow NaHS+H_2O$$

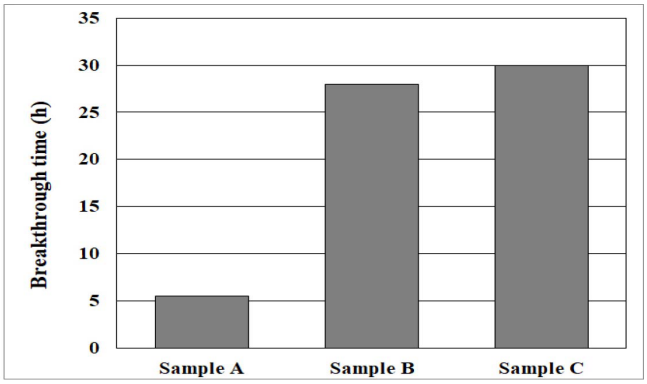

Fig. 4 Breakthrough time of sample studies.

Table 5 Chemical characteristics of alumina adsorbents

Components (wt%)	Al_2O_3	Na_2O	F	SiO_2	CaO	MgO
Sample A	95.01	0.21	0.01	0.01	2.76	1.84
Sample B	94.68	3.73	0.009	0.01	0.28	1.02
Sample C	95.11	3.98	0.065	0.101	0.188	0.31

The breakthrough time of the studied promoted alumina adsorbents (samples B and C) was measured after five sequential adsorption cycles to verify the stability of adsorbents after the regeneration process. The period of this stage for the pilot device was 12 hours, including 8 and 4 hours for heating and cooling steps, respectively. As observed from Table 6, the breakthrough time of Sample B decreases from 28 to 8.4 hours (about 70% of adsorption capacity) after five adsorption and desorption cycles, while the variations in the adsorption capacity of Sample C is negligible, and it is still stable after 5 sequential cycles. It is supposed that the lower BET surface area of sample C compared to sample B (see Table 3) reduces the possibility of green
oil formation on the adsorbent surface. Therefore, the pores of the former adsorbent are less occupied. The other reason for the durability of sample C can be the higher Na_2O content of this adsorbent (see Table 5), which reduces its catalytic activity; this subject will be discussed later.

To study the effect of the porosity of adsorbent on its stability and the possibility of regeneration, the nitrogen gas adsorption technique is applied on both fresh and used promoted alumina adsorbents (samples B and C), and the results are presented in Fig. 5 under the title of fresh and used adsorbents. The pore volume of fresh adsorbent B is higher than sample C, and it seems this type of promoted alumina can preserve high amounts of green oil in its mesopores. Consequently, it may acceptably resist fast deactivation. Analyses of used adsorbents after 5 cycles (see Fig. 5 under the title of Used adsorbent) prove that pores of adsorbent C are considerably free of green oil, and its pore volume only decreases from about 0.44 to 0.4 cm3/g, equal to about 10% reduction in volume of pores. In contrast, the mesopores of adsorbent B are severely filled with green oil, and about a 50% reduction in the volume of pores is observed. It is supposed that this intense green oil formation causes the fast deactivation of adsorbent B such that its breakthrough time decreases from 28 h in the first cycle to 8.4 h in the fifth cycle (see Table 6). Therefore, the pore volume of an alkaline adsorbent is not the main factor in preserving the stability and capacity of such adsorbents applied for removing H_2S from the olefinic gases. However, green oil formation during such a process is inevitable, and an adsorber should possess a minimum pore volume to hold the oligomerized hydrocarbons inside its structure without sacrificing the required specifications. Fig. 6 presents incremental pore volumes of fresh and used samples against pore radius. As seen, the structure of adsorbent C mostly contains meso pores with a radius of 50 to 80 A, whereas adsorbent B contains pores with a radius from 40 to 60 A. Due to the smaller pore diameter, the latter faces capillary condensation of unsaturated hydrocarbons in its structure, which are oligomerized during the regeneration process. Thus, the rate of side reactions and pore blockage in sample B is more intense than in sample C. It is inferred that adsorbent B contains small pores, which increases its specific surface area, and that contacting unsaturated molecules with its internal surface is plausible. Due to the low progress of side reactions in Sample C, the formation of green oil decreases, and therefore a longer lifetime for this adsorbent is expected. Analyses of the green oils formed on the surface and in the pores of samples B and C adsorbents confirm that these oligomers' mass ratio of carbon to hydrogen (C/H) is 6.97 and 6.92, respectively. It is concluded that the green oil formed in the pores of Sample C is lighter. Therefore, it can be removed more easily than sample B. Thus, the former adsorbent is regenerated more effectively at the same regeneration temperature. As shown in Figure 6, the undesired side reactions of pore blockage in sample B are much more severe than in sample C. The other noteworthy specification of adsorbent C, which preserves its stability against green oil and coke formation, is its acidity value [28-29], which decreases with sodium content [30-31]. Furthermore, the higher Na_2O content of adsorbent C (see Table 5) reduces its sulfate formation due to decreasing the acidity of the alumina surface and mitigating the catalytic activity of the surface to form sulfates [32-33].

Table 6 Breakthrough time for the regeneration experiments.

Studied samples	Unit	Cycle 1	Cycle 2	Cycle 3	Cycle 4	Cycle 5
Sample B	h	28	24.5	18.3	14.5	8.4
Sample C	h	30	29.5	29.1	29.2	29.1

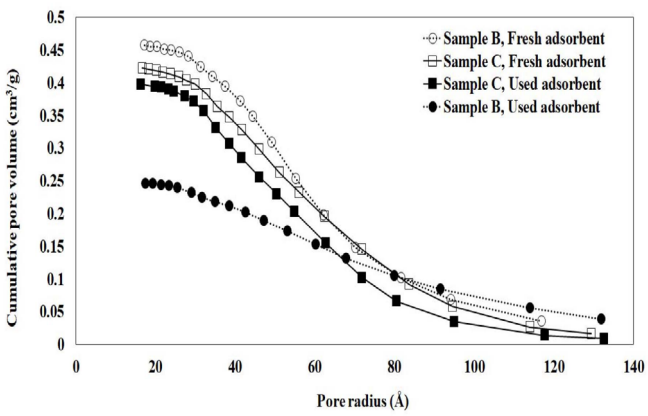

Fig. 5 Cumulative pore volume of fresh and used samples vs. pore radius (r) (Samples B and C).

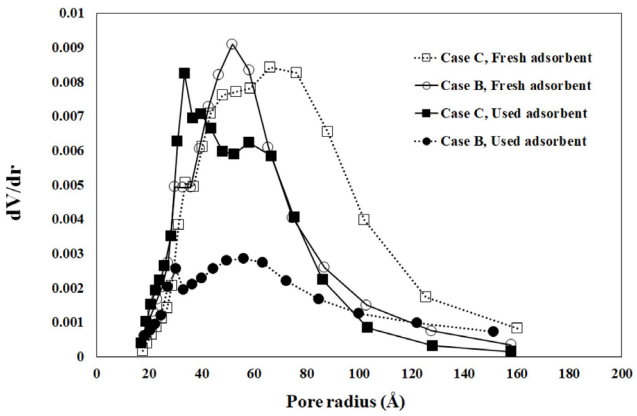

Fig. 6 Incremental pore volume (dV/dr) of fresh and used samples vs. pore radius (r) (Samples B and C).

Therefore, the reducibility of this promoted alumina with its regeneration time is superior to adsorbent B. It is obvious that side reactions in both adsorbents are unavoidable; however, the rate of these reactions can be minimized by adjusting pore size distribution and optimizing sodium content.

Conclusions

This research gives novel insights into the formation of green oil on the surface of different types of alumina adsorbents during the removal of hydrogen sulfide (H_2S) from the exhaust stream of the MTBE reactor. Furthermore, results confirmed that regular activated alumina did not have acceptable adsorption capacity for H2S removal, and therefore, the promoted alumina should be essentially employed for this application. Sodium oxide (Na_2O) content was the active element to intensify the adsorption of sulfur compounds on the alumina surface. Wide pores of the promoted alumina created fewer active sites for undesired side reactions, i.e., polymerization of C_3/C_4 unsaturated compounds. The adsorbent with a wider pore diameter faced less pore blockage during the regeneration step, and its life was prolonged. The acidic nature of the alumina was the main reason for the formation of green oil in the adsorption unit of the MTBE plant.

Acknowledgement

We would like to express our great appreciation to Seyed Sajad Mirian and Mahdi Asgari for their valuable and constructive suggestions during the planning and development of this research work.

References

1. Aguiar, M. F. & Coelho, L. V. (2017). Adsorption of sulfur compounds from natural gas by different adsorbents and desorption using supercritical CO2. Journal of Environmental Chemical Engineering, 5(5), 4353-4364, doi.org/10.1016/j.jece.2017.07.079.
2. Srivastav, A. & Srivastava, V. C. (2009), Adsorptive desulfurization by activated alumina. Journal of Hazardous Materials, 170 (2–3), 1133-1140, doi. org/10.1016/j.jhazmat.2009.05.088.
3. Santos, J. P. L., de Carvalho Lima Lobato, A. K., Moraes, C., de Lima Cunha, A., da Silva, G. F. & dos Santos L. C. L. (2016), Comparison of different processes for preventing deposition of elemental sulfur in natural gas pipelines: A review. Journal of Natural Gas Science & Engineering, 32, 364-372, doi.org/10.1016/j. jngse.2016.04.045.
4. Georgiadis, A. G., Charisiou, N. D. & Goula, M. A. (2020), Removal of hydrogen sulfide from various industrial gases: A review of the most promising adsorbing materials catalysts. Catalysts, 10 (5), 521-557, doi.org/10.3390/catal10050521.
5. Silveira, E. B., Veloso, C. O., Costa, A. L. H., Henriques, C. A., Zotin, F. M. Z., Paredes, M. L. I., Reis, R. A. Chiaro, S. X. (2015), Influence of metal oxides impregnated on silica-alumina in the removal of sulphur and nitrogen compounds from a hydrotreated diesel fuel stream. Adsorption Science and Technology, 33(2), 105-116, doi.org/10.1260/0263-6174.33.2.105.
6. Mehmood A., Alhasani H., Alamoodi N., Al Wahedi Y. F., Ibrahim S., Abhijeet R. & Nat J. (2020), An evaluation of kinetic models for the simulation of Claus reaction furnaces in sulfur recovery units under different feed conditions. Gas Science and Engineering, 74, 103-06, https://doi.org/10.1016/j.jngse.2019.103106.
7. Al-Degs, Y. S., El-Sheikh, A. H., Al Bakain, R. Z., Newman, A. P. & Al-Ghouti, M. A. (2016), Conventional and upcoming sulfur-cleaning technologies for petroleum fuel: A review. Energy Technology, 4(6):679-99, doi.org/10.1002/ente.201500475.
8. Fazlollahi, F., Asadizadeh, S., Khoshooei, M. A., Sardashti Birjandi, M. R. & Sarkari, M. (2021), Investigating efficiency improvement in sulfur recovery unit using process simulation and numerical modeling. Oil & Gas Science and Technology, 76, 18-27, doi. org/10.2516/ogst/2020093.
9. Weinlaender, C., Neubauer, R. & Hochenauer, C. (2018), Adsorptive hydrogen chloride and combined hydrogen chloride–hydrogen sulphide removal from biogas for solid oxide fuel cell application. Adsorption Science & Technology, 36(5-6), 1215-1232, doi. org/10.1177/0263617418772660.
10. Badra J., Alowaid F., Alhussaini A., Alnakhli A. & AlRamadan A. S. (2022), Understanding of the octane response of gasoline/MTBE blends. Fuel, 318, 123647, doi.org/10.1016/j.fuel.2022.123647.
11. Liu, J., Zhu, S., Zhang, L., Liu, Z., Cui, Q. & Wang, H. (2020), Study on Characterization and coke compositions of deactivated 5A molecular sieve for adsorption separation of industrial naphtha. Chemistry Select, 5, 12844-12852. Doi. 10.1002/slct.202002741.
12. Sun, H. & Shen, B. (2013), Experimental study on coking, deactivation, and regeneration of binderless 5A zeolite during 1-hexene adsorption. Adsorption, 19, 111-120, doi.10.1007/s10450-012-9426-y.
13. Masoudian, S. K., Sadighi, S., Abbasi, A., Salehrad, F. & Fazlollahi, A. (2013), Regeneration of a commercial catalyst for the dehydrogenation of isobutane to isobutene. Chemical Engineering technology. 36(9), 1593-1598, https://doi.org/10.1002/ceat.201300090.
14. Ejtemaei, M., Sadighi, S., Rashidzadeh, M., Khorram, S., Back, J., Delir Kheyrollahi Nezhad, P., Penner, S., Noisternig, M. F., Salari, D. & Niaei, A. (2022), Effect of O2/N2 glow discharge plasma on zeolite extrudates as water adsorbent. Chemical Engineering and Processing-Process Intensification, 181, 1-44, doi.org/10.1016/j. cep.2022.109084.
15. Ejtemaei, M., Sadighi, S., Rashidzadeh, M., Khorram, S., Back, J., Penner, S., Noisternig, M. F., Salari, D. & Niaei, A. (2022), Investigating the cold plasma surface modification of kaolin- and attapulgite-bound zeolite A. Journal of Industrial and Engineering Chemistry, 106, 113-127, doi.org/10.1016/j.jiec.2021.10.020.
16. Siakavelas, G.I., Georgiadis, A.G., Charisiou, N.D., Yentekakis, I.Y., Goula, M.A. (2021), Cost-effective adsorption of oxidative coupling-derived ethylene using a molecular sieve. Chemical Engineering and Technology. 44, 2041-2048, doi.org/10.1002/ceat.202100147.
17. Overjero, G., Romero, M. D., Diez, D., Mestanza, M. & Diez, E. (2020), Bentonite as an alternative adsorbent for

the purification of styrene monomer: Adsorption kinetics, equilibrium and process design. Adsorption Science & Technology, 28(2), 101-123, doi.org/10.1260/0263-6174.28.2.101.
18. Coelho, A., Caeiro, G., Lemos, M. A. N. D. A., Lemos, F. & Ribeiro, F. R. (2013), 1-Butene oligomerization over ZSM-5 zeolite: Part 1 – Effect of reaction conditions. Fuel, 111, 449-460, doi.org/10.1016/j.fuel.2013.03.066.
19. Corma, A., Martínez, C. & Doskocil, E. (2013), Designing MFI-based catalysts with improved catalyst life for C3= and C5= oligomerization to high-quality liquid fuels. Journal of Catalysis, 300, 183-196, dx.doi.org/10.1016/j.jcat.2012.12.029.
20. Rezaei S., Shafaghat H. & Daud W. (2014), Production of green aromatics and olefins by catalytic cracking of oxygenate compounds derived from biomass pyrolysis: A review. Applied Catalysis A: General, 469, 490-511, doi.org/10.1016/j.apcata.2013.09.036.
21. Lu, Y., Yan, Q., Han, J., Cao, B., Street, J. & Yu, F. (2017), Fischer–Tropsch synthesis of olefin-rich liquid hydrocarbons from biomass-derived syngas over carbon-encapsulated iron carbide/iron nanoparticles catalyst. Fuel, 193, 369-384, https://doi.org/10.1016/j.fuel.2016.12.061.
22. Lamberov, A. A. & Sitnikova, E. Y. (2009), Experience of the industrial use of alumina and KA zeolite in the processes of drying of olefin-containing mixtures in petrochemical industry, Petroleum Chemistry, 49, 184-187, doi.org/10.1134/S0965544109020121.
23. Masoudi-Nejad, M., Fatemi, S. (2014), Thermodynamic adsorption data of CH4, C2H6, C2H4 as the OCM process hydrocarbons on SAPO-34 molecular sieve. Journal of Industrial and Engineering Chemistry. 20, 4045-4053, doi.org/10.1016/j.jiec.2013.12.107.
24. Elmutasim, O., Basina, G., Al Shami, D., Gaber, D., Gaber, S., Karanikolos, G. N., Al Wahedi, Y. (2020), On the impact of copper local environment on hydrogen sulfide adsorption within microporous AlPO4-5. Journal of Environmental Chemical Engineering, 8 (5), 104245, doi.org/10.1016/j.jece.2020.104245.
25. Amvrosios G.G., Nikolaos D.C, Goula, M.A. (2020), Removal of hydrogen sulfide from various industrial gases: A review of the most promising adsorbing materials. Catalysts, 10, 5, 521-557, doi.org/10.3390/catal10050521.
26. De la Osa, A.R., De Lucas, A., Valverde, J.L., Romero, A., Monteagudo, I., Coca, P., Sanchez, P. (2011), Influence of alkali promoters on synthetic diesel production over Co catalyst. Catalysis Today, 167(1), 96-106, doi.org/10.1016/j.cattod.2010.11.064.
27. Bagreev, A. & Bandosz, T. J. (2002), A Role of sodium hydroxide in the process of hydrogen sulfide adsorption/oxidation on caustic-impregnated activated carbons. Industrial Engineering & Chemical Research, 41, 672-679, doi.org/10.1021/ie010599r.
28. Moslempour, Z., Sadighi, S., Dashti, A. & Ahmadpour, A. (2021), Investigating the properties and performance of 3A molecular sieves as an adsorbent to prevent coke formation in olefin dehydration process. International Journal of Chemical Reactor Engineering, 20(8), 833-843, doi.org/10.1515/ijcre-2021-0179.
29. Rezaei, P. S., Shafaghat, H. & Ashri Wan Daud, W. M. (2014), Production of green aromatics and olefins by catalytic cracking of oxygenate compounds derived from biomass pyrolysis: A review. Applied Catalysis A: General, 469, 490-511, doi.org/10.1016/j.apcata.2013.09.036.
30. Hashiba, T., Hayashi, D., Katada, N. & Niwa, M. (2004), Decrease of catalytic activity and solid acidity by ion exchange of Na cation on HZSM-5. Catalysis Today, 97(1), 35-39, doi.org/10.1016/j.cattod.2004.04.051.
31. Gayubo, A. G., Alonso, A., Valle, B., Aguayo, A. T. & Bilbao, J. (2010), Selective production of olefins from bioethanol on HZSM-5 zeolite catalysts treated with NaOH. Applied Catalysis B: Environmental, 97(1–2), 299-306, doi.org/10.1016/j.apcatb.2010.04.021.
32. Laperdrix, E., Sahibed-dine, A., Costentin G., Saur O., Bensitel M., Nédez C., Mohamed Saad A. B., Lavalley J. C. (2000), Reduction of sulfate species by H2S on different metal oxides and promoted aluminas. Applied Catalysis B: Environmental. 26(2), 71-80, doi.org/10.1016/S0926-3373(00)00108-9.
33. Mitchell, M.B., Sheinker, V.N. (1996), Adsorption and reaction of sulfur dioxide on alumina and sodium-impregnated alumina. The Journal of Physical Chemistry, 100, 7550-7557, doi.org/10.1021/jp9519225.